Acknowledgements

First and foremost I would like to thank my academic supervisor, Professor Yusuf Altintas for giving me the opportunity to conduct research alongside his team and for his guidance throughout this project.

I am especially grateful to Nima Dabiri, research engineer at the Manufacturing and Automation Laboratory, for his continuous supervision, insightful advices and ongoing support throughout this study.

Additionally, I would like to thank the entire team for their warm welcome and for fostering a comfortable and motivating work environment.

Finally, I wish to thank Dr. Behnam Karimi for welcoming me into his project and guiding me in our work on blade machining.

Contents

List of Figures

List of Tables

Introduction

A leading field in the international industry, manufacturing has long attracted the attention of researchers. Today, more than ever, the rapid evolution of technology demands continuous improvement of manufacturing processes, especially those involving material removal. One of the greatest challenges in machining is meeting increasingly tighter tolerances and achieving excellent surface finishes.

To resolve these issues, it is essential to study the vibratory phenomena that occur during the material cutting process. Vibrations and chatter prediction enables machinists and engineers to select stable cutting conditions. This not only improves surface finish and dimensional accuracy, but also significantly reduces tool wear, risk of breakage, and machine downtime, leading to more efficient and reliable manufacturing. However, vibrations and chatter depend on a multitude of different parameters, being difficult to predict.

Machine tool vibrations research is a large field opening a wide range of research opportunities. As early as 1961, Tobias S.A. engaged in the study of machine tool vibrations [Tobias, 1961]. Since then, studies suggested a method to calculate the limiting depth of cut for turning [Altintas and Weck, 2004] and stability lobes [Altintaş and Budak, 1995]. Despite decades of research, the field remains rich with further explorations and topics to be explored

In this context, the Manufacturing and Automation Laboratory played a crucial role in advancing research in the field of machine vibrations and was source of numerous publications, establishing itself as a leader in the domain.

During several decades of work on making vibration and chatter simulation accessible to companies, the lab developed ergonomic software and spread research knowledge.

Joining the laboratory from May 1st to August 22nd 2025, my mission was to simulate and optimize a machining process by performing finite element analysis on a thin-walled structure. Major stakes are to increase productivity by reducing machining time, minimize tool wear and improve surface finish, all while ensuring chatter stability.

First, a conventional approach will be adopted, and the impact of the workpiece geometry on vibrations and chatter stability will be studied. Subsequently, a waterline strategy will be employed and optimized with the aid of finite element analysis.

Chapter 1

Introduction to the laboratory and work conditions

This first chapter is an introduction to life in Vancouver and working habits in the laboratory.

Contents

1 The Manufacturing and Automation Laboratory in Vancouver

1.1 The Manufacturing and Automation Laboratory (MAL)

The Manufacturing and Automation Laboratory, located 2225 Eastmall, British-Columbia, Vancouver, Canada, is part of the University of British Columbia.
Around twenty people work there, including professors, PhD students, postdoctoral researchers, engineers and interns.

The laboratory occupies premises in three buildings: High-head, Rusty hut and Kaiser building. It actually operates two Mori-Seiki milling machines, namely a DMU 50 and a recently acquired NXT 1000, which both support advanced machining capabilities.

Figure 1.1: Photo of the High head building

Research is conducted in the mechanics and dynamics of metal cutting operations, spindle design and analysis, micro-machining, virtual simulation of machining operations and CNC machine tools, design and digital control of high speed feed drives, precision machining, sensor assisted intelligence machining and chatter stability of cutting processes.

Different software were created by the laboratory. First, CutPro, designed for achieving the highest possible material removal rates, extended tool life, and increased spindle life. Then NPro, a Siemens NX CAM integrated machining optimization tool. Last, MachPro, the most advanced process simulation and NC program optimization software.
These technological innovations contribute to the university's reputation and reflect the region's commitment to both industrial excellence and innovation.

1.2 Vancouver

Vancouver, where many scientific advancements take place, is a multicultural city on the west coast of Canada (see aerial photo below). It was build on a rainforest in 1886 and is now the most crowded city in British-Columbia and the third urban area in Canada after Toronto and Montreal.

Figure 1.2: Aerial photo of Downtown district, Vancouver from https://vancouver.ca

Next to the Rocky mountains, the options for hiking in the region are countless. Cities north of Vancouver such as Squamish and Whistler have a worldwide reputation for ski resorts, climbing spots and mountain biking routes, drawing athletes from all over the world. Hence, the culture of sport is very developed in British-Columbia, even inside Vancouver with ice hockey, soccer or baseball. Vancouver even hosted the Winter Olympic Games in 2010, strengthening its international reputation.

Forestry is the largest industry of the city, followed by tourism. Due to a high quality of life and a urban center surrounded nature, the attractiveness of the city is very high, drawing fortunate people from all over the globe, sharply increasing real estate prices. Moreover, the major film studios located in Vancouver and Burnaby have transformed the region into one of the largest film production hubs in North America, earning the nickname 'Hollywood North'.

2 Work environment

During my internship, I was supervised by Nima Dabiri, engineer in mechanics, under the official supervision of Professor Yusuf Altintas. My working hours were from 9am to 4:30pm with a 30 minutes lunch break. The beginning and ending hours are flexible as long as the total effective hours per week is 35. The fact of not having intermediate breaks in the morning and afternoon was not very noticeable but represented a precious daily gain of time.

Security and prevention is a highly important matter inside UBC (University of British Columbia). Every on-boarding student, visitor or employee has to take prevention courses in themes like sexual misconducts or cybersecurity basics as well as a safety visit of the laboratory building if applicable. Safety protection equipments might also be mandatory.

Concerning transit, the city is well deserved with a wide bus and train network. However, I made the choice of buying a bike for commuting, with a 50 minutes ride per day, faster than the 80 minutes per day of bus transit. To travel north, busses and sea-busses are available and give access to many trail starts. For more distant journeys, car-sharing options are widespread and affordable.

Chapter 2

Thin-walled part machining

In this chapter, issues encountered when machining thin-walled parts will be studied. Solutions will also be implemented to both optimize the cutting process and reduce previous problems.

Contents

1 Design

Vibrations and chatter in milling operations have been studied by researchers for over sixty years [Tobias, 1961], mainly exploring tools deflections.
However, it is not always sufficient to rely only on the tool to predict vibrations. In fact, thin walled part such as turbine blades also require to consider the workpiece as flexible. Therefore, both flexibilities of the tool and the workpiece have to be taken into consideration when predicting vibrations and chatter.

In order to investigate the impact of the workpiece geometry on chatter stability, I designed a parametric thin-walled part on NX, a Computer Aided Manufacturing (CAM) software developed by Siemens.
The main idea of the part is to check where vibrations and/or chatter will occur. Therefore, I designed different geometries made of open and closed thin walls of 1 mm thickness, as well as 5 axis shapes (see figure 2.1 below). The thin wall machining refers to cases where the height-to-thickness ratio exceeds 8. In our case, the ratio is 33.

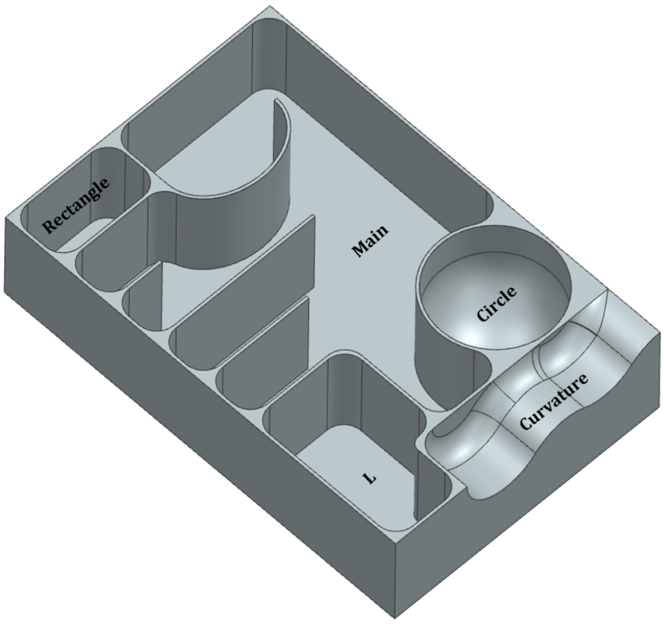

Figure 2.1: ISO view of my thin-walled part design with region labels

One of the most critical parameters to consider when optimizing a milling process is the width of cut. Increasing it not only leads to an improvement in productivity but also amplifies the risk of chatter. In features such as pocketing, this parameter is not controllable and varies along the path. The use of the adaptive milling feature instead of pocketing is thus strategic. It allows the radial engagement to be kept constant all over the path by adding a rotation to the tool motion. This property will be valuable when adjusting cutting conditions.

2 Conventional approach

The common strategy to machine a part is the conventional approach. It is defined by a single sequence of roughing, semi-finishing, and finishing, with the depth of cut determined by the maximum plunging capacity of the tool. This strategy only considers the tool flexibility, which constitutes a strong assumption. To evaluate the limitations of this method, the thin-walled part was initially machined using the conventional approach.

2.1 Tap testing and tool tip FRF of milling tools

In this subsection, we focus on tap testing and the Frequency Response Functions (FRFs) at the tool tips of spindle-holder-tools assemblies in a milling machine. Tap tests are used for identifying the mode shapes, damping ratio and natural frequencies of the structure to create an FRF:

$$\mathrm{FRF(f)} = \left(\frac{\text{FFT of output(f)}}{\text{FFT of input(f)}}\right)$$

Although the workpiece in this study was designed with thin walls, we initially assume it to be rigid for simplification. This assumption, however, is not valid. Yang Ding and Lida Zhu [Ding and Zhu, 2018] used finite element analysis to model time-varying dynamics of the workpiece due to material removal. They Demonstrated how both tool and workpiece flexibilities affect stability lobes.

Before beginning any test, it is necessary to ensure that the impact of experimental variables is minimized. These variables can include ambient temperature, sensor placement, or input force locations on the tool.

Once external factors are optimized, the dynamic behaviour of the machining system itself comes into focus. In high-speed machining, balancing tools is crucial to minimize vibrations and ensure measurement accuracy. An unbalanced tool can introduce parasitic vibrations, which may hide or distort the real structural response during modal testing.

The procedure to balance tools consists in screwing small inserts into the tool holder. The location where the inserts are needed is given by a machine that rotates the tool and tool holder at a thousand rounds per minute. Once the tool is balanced and mounted in the milling machine, an impact device must be chosen. Shakers offer a better accuracy than hammers but take longer to set up, which is why they are not used in the laboratory.

A big hammer will generate a waveform of high magnitude and duration to excite bigger structures and catch lower frequencies. In this study, the modes that have to be excited are the ones corresponding to the tools, tool-holders and spindle. A medium-sized hammer is therefore sufficient. In addition, the choice of the tip is important. A softer tip typically made of rubber will excite less frequencies than a hard one made of stainless steel for example. However, risks of double hits are more important with harder tips.

The ideal procedure would be to first hit with a soft tip. If CutPro detects a mode that could not be characterized sufficiently because of a lack of excitation energy, a harder tip can be employed. In the case of this study, only a general identification of the modes is required. Therefore, only a soft tip was used, and the cutting conditions were reduced by 30% as a security.

The choice of an accelerometer should be done in accordance with the hammer characteristics. Small accelerometers are mainly sensible to higher frequencies and add less mass to the structure, providing more accuracy [Özşahin et al., 2010]. On the contrary, bigger accelerometers can identify lower frequencies by exciting larger structures.

In this study, the sensor sensitivities were the following: 2.248mv/N for the Dytran 5800B4 hammer and 9.4mV/g for the Dytran 3225F1 accelerometer. These values were entered in CutPro before the tap test.

Impact tests were conducted in two directions to capture potential axial asymmetries of the machine. The accelerometer is mounted on the tool tip using wax. Each measurement session is preceded by a single calibration impact. This allows the data acquisition system to dedicate memory slots for measurement prior to the test.

Figure 2.2: Tap testing setup

When proceeding to the test, an average is calculated over five hits performed perpendicularly to the z direction and on the opposite side of the accelerometer. The main issues that can be faced during a tap test are double hits and discrepancies about the magnitude and location of the impact force for the five hits. These sources of error can be handled by applying a security coefficient on the results.

2.2 Stability lobes

A tool stability lobes diagram depends on tool geometry [Tehranizadeh et al., 2022], tool dynamics (stiffness K, damping ratio ζ, natural frequencies f_n) and material. Two graph types are commonly used: stability lobes, to choose spindle speeds, and radial stability at a certain spindle speed to select depths and widths of cut.

In the absence of knowledge regarding stability lobes, depth of cut is typically reduced whenever chatter occurs. A reduction in spindle speed does not necessarily result in stable cutting conditions, whereas decreasing the depth of cut to a sufficiently low value guarantees stability regardless of spindle speed. However, this approach leads to a significant reduction in productivity. On the contrary, knowledge of stability lobes enables the identification of spindle speed values at which cutting becomes stable, potentially allowing an increase in both spindle speed and depth of cut. An understanding of vibrations and chatter in machining is therefore essential for achieving stable cutting conditions while increasing productivity.

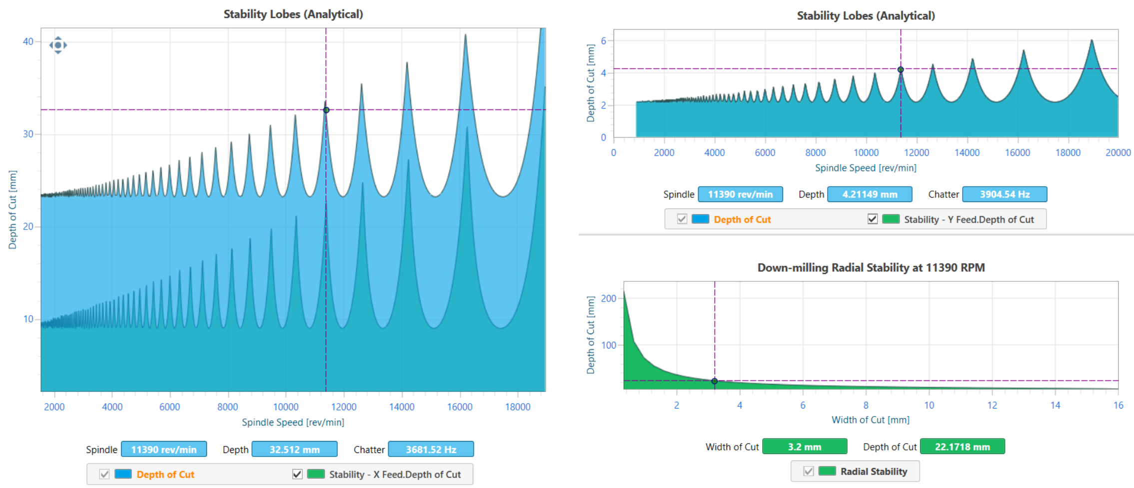

Figure 2.3: Stability lobes diagram

Nevertheless, minimizing chatter is not only a matter of efficiency and quality. It also has significant environmental benefits. According to the Advanced Manufacturing Research Centre at the University of Sheffield: 'Chatter means excess energy consumption, resulting in higher operating costs and increased carbon emissions.'

More rigorously, stability lobes are three-dimensional diagrams, where the third axis typically represents radial engagement. This dimension plays a crucial role because the direction of cut affects the orientation of cutting forces, which in turn influences the dynamic behaviour of the system. To account for this, one can discretize the radial engagement angle between 0 and 90 degrees, and superimpose multiple stability lobes diagrams, each corresponding to a different cutting direction. This approach enables the identification of optimal cutting conditions that ensure both stability and high productivity across all directions of cut.

An important point to consider is the non-linear relation between depth of cut and width of cut. Specifically, as the width of cut decreases, the maximum admissible depth of cut grows exponentially. This implies that keeping a small width of cut can significantly increase productivity by allowing deeper stable cuts.

Nonetheless, at low cutting speeds, process damping can attenuate high-frequency chatter modes. This phenomenon occurs when the relief face of the tool rubs against the sinusoidal shaped surface left by previous vibrations of the tool. This rubbing flattens out the high frequency oscillations, preventing their excitation.

Although the signal from FRF (Frequency Response Function) is usable, modes are not clearly distinguishable. Modal analysis is a procedure used to clean FRF signals. The option implemented in CutPro includes an algorithm that finds peaks that correspond to natural frequencies. The user can select peak locations he finds relevant to consider and the software performs a curve fitting.

To get access to stability lobes, material properties and tool geometry and dynamics must first be defined. Uploading modal data files previously created with modal analysis informs the software of the dynamics of the tool. To get a first insight, material can be considered rigid. Lastly, an intuitive feed rate and a max spindle speed must be completed in the appropriate boxes, and the cutting method must be chosen (down milling in this study).

The choice of cutting conditions follows the general procedure defined hereafter:

1. Set radial depth of cut to a slotting value (100% of tool diameter), to be as conservative as possible, with radial stability option disabled ;

2. Start the simulation and choose a stable spindle speed ;

3. Enable radial stability and enter the chosen spindle speed before running again ;

4. Fix a desired depth of cut and select a radial engagement that allows it ;

5. Enter the radial engagement value in the radial depth of cut menu, disable radial stability and run again to verify the spindle speed.

If operations have been previously carried out in the same cutting area, stocks will have been defined, meaning that the remaining depth and/or width to cut will be already a simulation input. In that case, only the first step of the procedure is required.

In roughing operations, surface finish is not important and time can be saved by optimizing the feed rate. Based on the chip thinning phenomenon and given the relationship between chip thickness h and desired feed rate c:

$$h = c\sin(\varphi)\sin(\kappa_R)$$

The optimal feed rate can be calculated from the width of cut b an the cutting edge angle κ_R as follows:

$$c = \frac{h}{\sin\left(\pi - \arccos\left(\frac{r_{\text{tool}} - b}{r_{\text{tool}}}\right)\right)\sin(\kappa_R)}$$

For semi-finishing and finishing operations, the desired feed rate is conserved to prioritize a better surface finish.

The impact of feed rate on stability lobes is negligible, so it is not compulsory to iterate the simulation based on this new feed rate value.

This process has to be performed for all tools.

2.3 Machining and observations

The machining operations were performed using the following tools:

- A 2-flute 16mm diameter flat endmill for roughing ;
- A 2-flute 10mm diameter flat endmill for walls finishing and circle-and-curvature semi-finishings ;
- A 2-flute 12mm diameter ball endmill for circle and curvature semi-finishings and finishings.

The machine was a 5 axis DMU 50 from Mori Seiki. The workpiece material was aluminum alloy Al7050-T7451. Tools were mounted using HSK type holders.

Property	$\rho\,(kg/m^3)$	$E\,(MPa)$	ν
Value	2800	71700	0.3

Table 2.1: Al7050-T7451 properties

The stable cutting parameters chosen with tools stability lobes were the following:

Cutting condition	D16N2 flat endmill	D10N2 flat endmill		D12N2 ball endmill
		semi-finishing	finishing	
Spindle speed [RPM]	11390	18180	18340	18990
Depth of cut [mm]	16.5	2.5	11	0.2
Width of cut [mm]	3.2	8	0.1	0.3
Feed per flute [mm/flute]	0.124	0.05	0.05	0.05

Figure 2.4: Cutting conditions

The idea in machining this part was to observe potential chatter. In order to better analyze this phenomenon, different parameters were measured during machining. First, a dynamometer was placed under the vice to collect xyz forces. Additionally, a data set was directly collected from the machine and acquired with Intelcut: xyz current, spindle speed, current and torque, feedrate and xyz positions. Last, a microphone set up inside the machine gave access to the sound values. The problem that was faced when using this device was the presence of lubricant, which is necessary for machining aluminum, whose splashes produced a parasitic sound.

The total cycle time was 2274.94 seconds and the result was the following:

Figure 2.5: Machined thin-walled part

Although the floor of the part has a poor surface finish, this region is not important for this study. As it can observed on figure 2.6 and in Appendix B, most of the part was prone to chatter, leaving marks on walls.

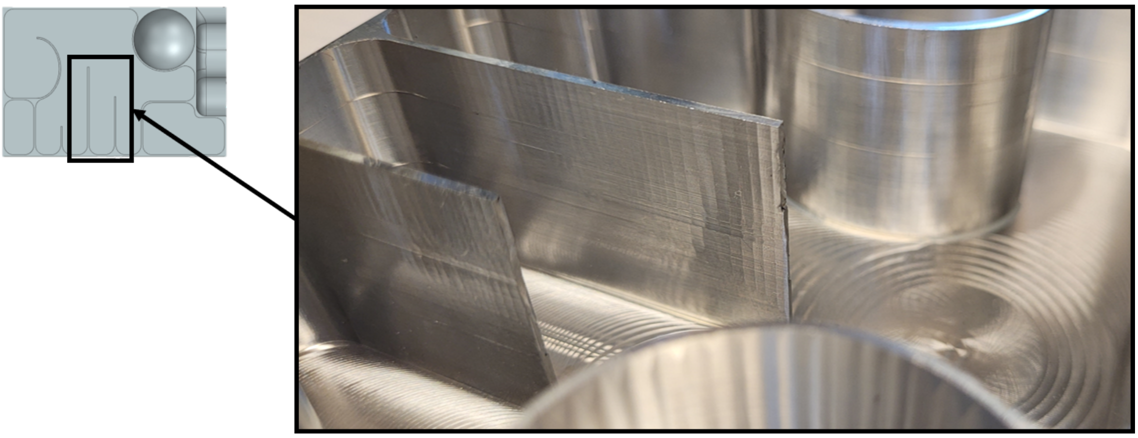

Figure 2.6: Chatter marks

The FFT in the previously highlighted wall location was identified with the output data from the experiment:

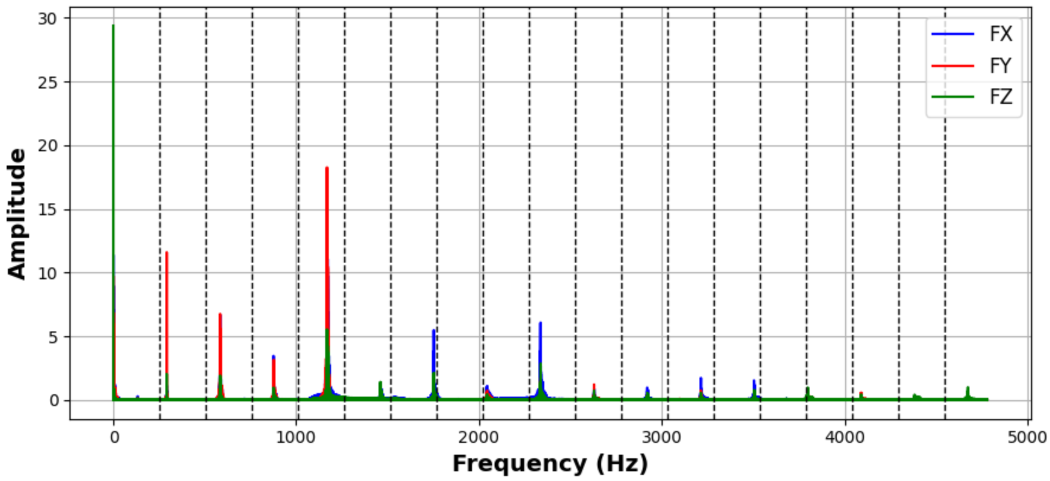

Figure 2.7: FFT from machining outputs on the long walls location

Chatter follows recognizable patterns that can be detected on the FFT: the chatter peak frequency is always very close to a multiple of the spindle frequency and is never equal to it. On the figure above, the chatter frequency can be spot at 1150Hz. The other chatter marks locations and associated FFTs are presented in Appendix B.

Given the large amount of chatter frequencies distributed in different locations of the cut, manually avoiding them would be impractical. A more efficient solution is the waterline approach.

3 Machining optimization - waterline approach

3.1 Time optimization

Machining times given by CAM software are not accurate. This is due to the fact that software ignore machine characteristics and consider the feedrate to be as intended for every operation during machining. In reality, machines need a certain time to reach intended feerates depending on their acceleration and jerk characteristics. Real machining time are thus usually greater than simulated.

Machpro is a software developed by the MAL to optimize productivity. By uploading the CAM file, defining the material of the workpiece and the characteristics of the machine, users are able to perform improvements in the machining process. Therefore, it is, for example, possible to optimize the process by defining a threshold on the chip load (also named feed per tooth). When this threshold is exceeded, the chip load is reduced, and vice versa.

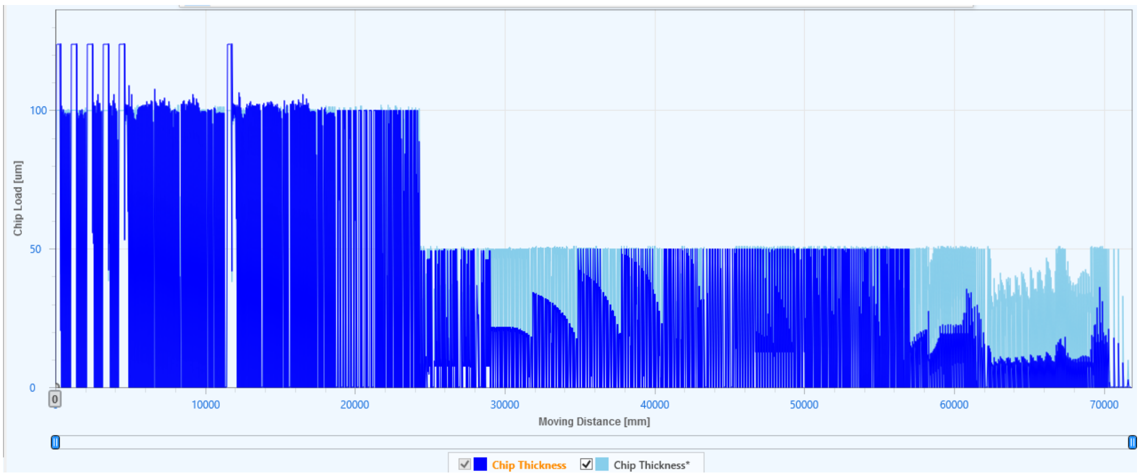

Figure 2.8: Machining optimization with MachPro

After applying a threshold of 0.1mm on the chip load, the time grew from 38 minutes before optimization up to 42 minutes after. The reason of this result is the following. The feedrate was reduced in roughing operations and increased in finishing operations. However, the machine could already not reach the intended feedrate, which means that increasing it could not change anything. As a result, the machining time was increased.

3.2 Chatter avoidance

3.2.1 Waterline approach introduction

To avoid chatter, the waterline approach can be implemented in the CAM process. This consists of alternating roughing and finishing operations with shallow depths of cut in order to gradually increase the stiffness of the part in the cutting zone. The main objective is to ensure that the tool is more flexible than the workpiece to better manage the process. In fact, if the stiffness of the part is increased, its modal frequencies will also increase, following the relation $\omega = \sqrt{\frac{k}{m}}$. If the workpiece modes are high enough, the cutting process might predominantly excite the modes of the tool rather than those of the workpiece.

In the waterline machining approach, the same tool must be used for all operations; in this case, a $10mm$ diameter flat end mill was employed. The downside of the method is an increase in the machining time. For this reason, a compromise must be done between stability and productivity. A conservative approach is usually adopted to choose a depth of cut allowing a low height-over-thickness ratio on the walls, which is not efficient.

The purpose of this study is to find the optimal ratio not only to be able to apply the waterline approach but also to ensure improved productivity.

A solution to meet with this challenge would be to perform a complete FEA considering the real time stiffness change of the workpiece over time. Such a method would be highly time consuming and computationally inefficient. Therefore, another approach was adopted. First, a depth of cut is chosen based on the tool properties. Then, by using uniform passes, FEA is performed on each waterline step to assess stability.

3.2.2 Workpiece Finite Element Analysis (FEA) and Part Tap Tests

In order to assess stability at each waterline steps, the workpiece must first be considered flexible and its natural frequencies identified. On the tool, the FRF is constant so a tap test is sufficient. on the workpiece however, it is not easy to tap test because the FRF changes for different locations due to mode shapes. Getting FRFs would require to machine a pass, then tap test and reiterate, which is not practical. The solution lies in Finite Element Analysis (FEA). An accurate model can help predict vibrations at each cutting step, allowing a depth of cut tuning for the waterline approach. However, the structural damping of the part is unknown and has to be identified.

Tap testing the part gives access to the part FRF on modes locations. By iterating FEA simulations and comparing the results with experimental data, the structural damping previously chosen can be tuned.

It is important to note that the workpiece stiffness is variable during the cut because of the change in mass induced by chip removal. A recalculation of stability lobes and the choice of stable cutting conditions should thus be done at every step of the cut to ensure a better stability all along the cut. To simplify the analysis, this variation of mass is neglected.

The first main step of the FEA model is the mesh choice. To meet with this challenge, an iterative meshing procedure was employed by first using a coarse meshing to locate modes, then refining globally and finally refining on modes locations until convergence of the natural frequencies was achieved (see figure 2.9).

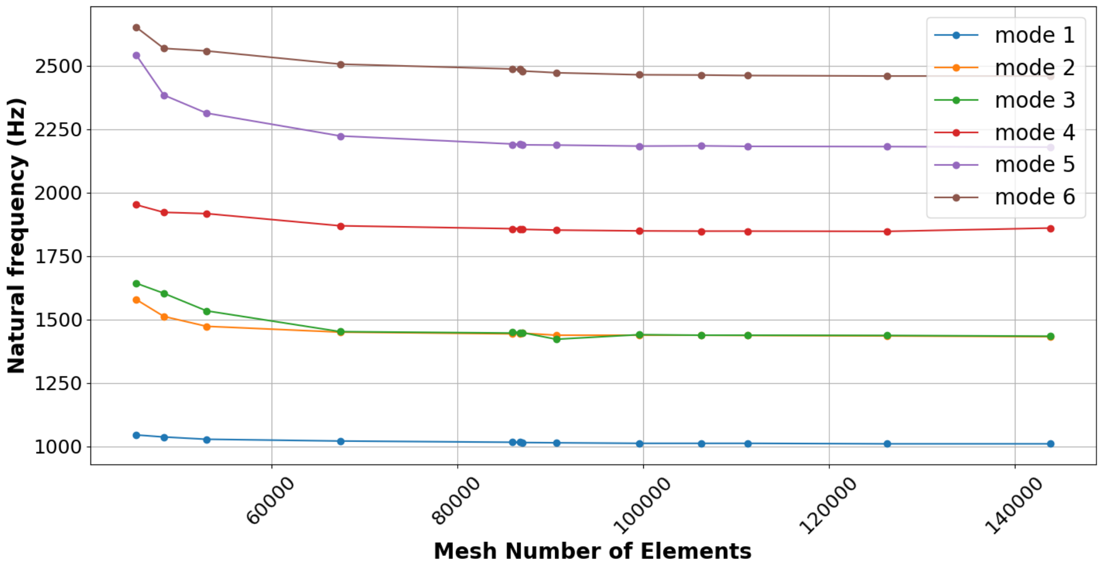

Figure 2.9: FEA convergence

Convergence was achieved around 100,000 number of elements. The thin-walled part was finally meshed using tetrahedral elements, with a global element size of 5mm, and local refinement to 1mm around boundary constraints and studied modes locations. The material assigned to the part was Al7050-T7451.

Concerning the boundary conditions, the part was initially constrained with an encastrement on the side and bottom surfaces to simulate clamping via support blocks and a vice. However, the support blocks did not contact the part during the tap test experiment due to the vice clamping. To address this issue, the FEA model was adjusted by removing the bottom face encastrement.

Because the results matching was not satisfactory, the decision was made to use high stiffness springs in order to model the vice clamping instead of the encastrement. The stiffness of the spring in the normal direction to the vice jaws was set to $2000N/mm$. In the two other orthogonal directions, a friction coefficient of 0.3 was considered.

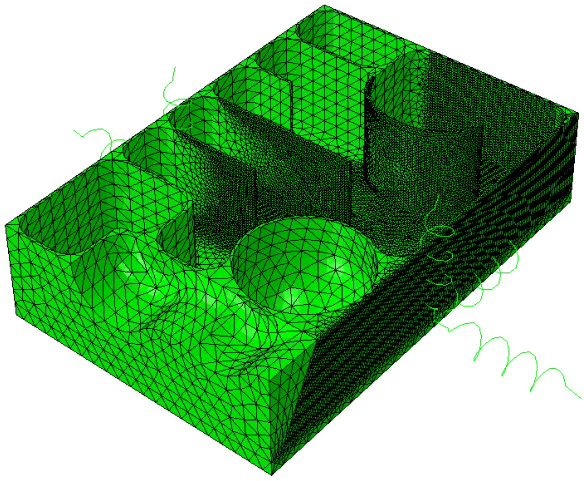

Figure 2.10: Part mesh with local refinement and spring boundaries

A free-free modal analysis then revealed the exact same results as with the springs boundary conditions. To meet with this problematic of clamping stiffness definition, a new boundary condition solution came into place. Using two sheet parts, defining a contact between these parts and the workpiece and fixing the sheets to the ground enabled vice clamping modelling.

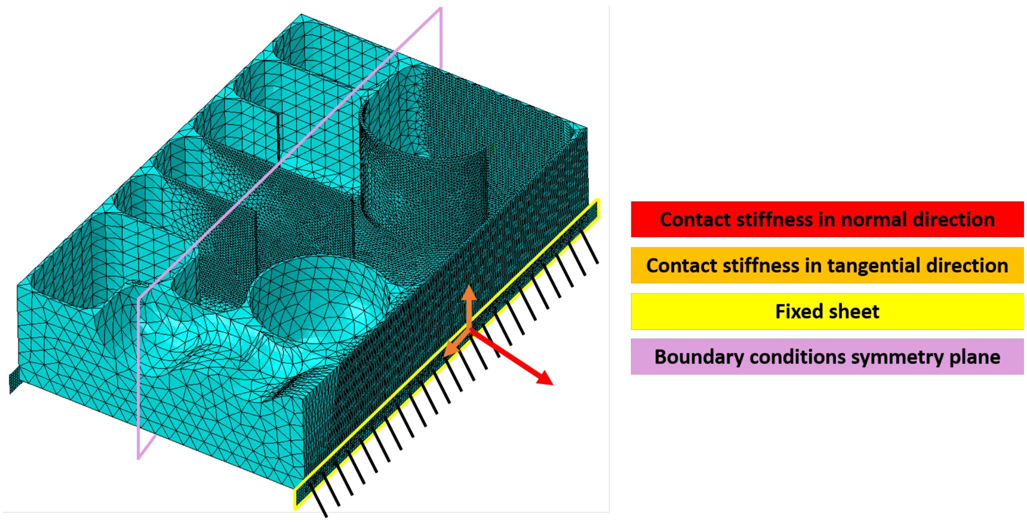

Figure 2.11: Contact boundary conditions and mesh

In the normal direction of the contact, a stiffness had to be defined whereas in the tangential direction, a friction coefficient could be chosen. The hypothesis was made that the friction coefficient is equal to 0.3.

A tuning of the contact stiffness was then processed, giving the following results:

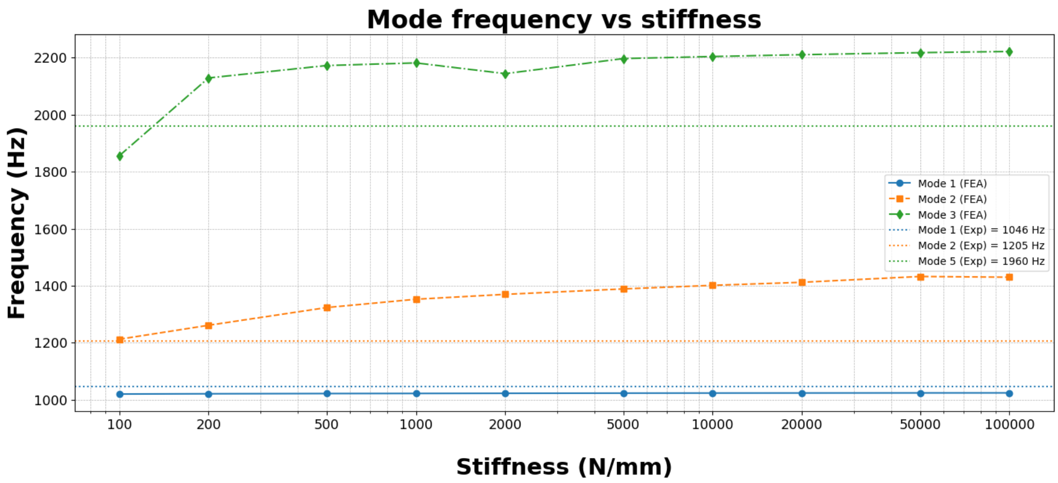

Figure 2.12: Clamping stiffness tuning

The choice of a $5000N/mm$ stiffness was made to model the vice clamping. Although lower stiffness values seem better to match experimental results, their results reveal that multiple modes appear on the same location next to each other, which is not representative of the tap test results.

To identify the structural damping, tap tests were conducted on locations corresponding to modes 1, 2 and 5, as referenced in Appendix C. Achieving single hits by using an impact hammer on a thin wall is impossible. Instead, an automatic impact hammer and a laser velocity sensor can be used.

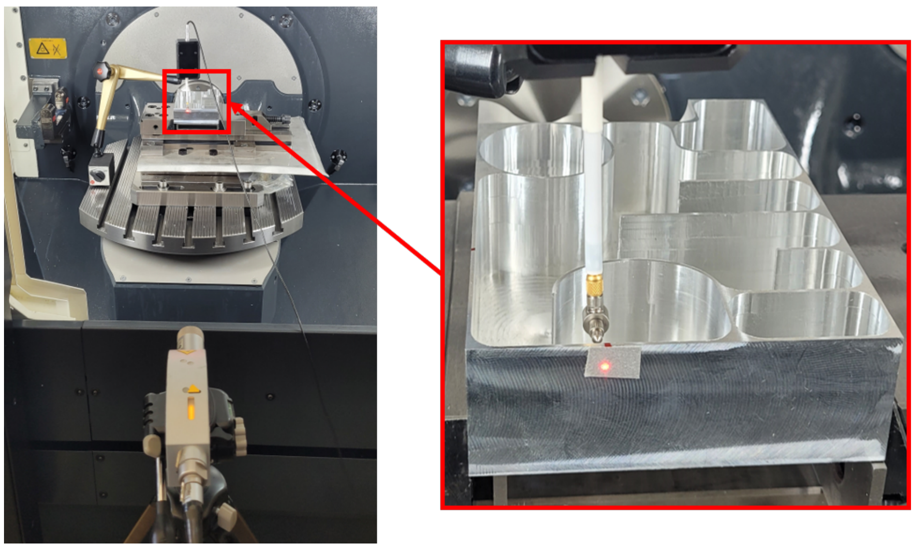

Figure 2.13: Automatic tap test setup

With an automatic hammer, the magnitude and duration of the hit can be selected to avoid double hits. However, due to the high height-over-thickness ratio of the walls (33), double hits still occurred. These double hits were disregarded, as their impact on the modes are slight, and data were collected.

By comparing results with FEA simulations, the structural damping was tuned iteratively by making the assumption that the structural damping is the same for each mode (cf. Appendix D).The first mode location was selected as the reference, as it represents the most critical zone. This mode corresponds to the lowest natural frequency, indicating that the associated wall is the most flexible. Once matching the experiments, the FEA model was used to simulate the waterline approach at each step.

3.2.3 FEA-based waterline approach

In order to minimize the amount of FEA simulations and save time, the depth of cut was chosen as 11mm, resulting in three steps as highlighted in the figure 2.14.
To ensure that the part is more rigid than the tool, the roughing operation was set to leave 1mm stock. For this operation, the tool is thus flexible and the workpiece is considered rigid.
Then, a semi-finishing leaves 0.1mm as a stock for the finishing operation. During these two last operations, both the tool and the workpiece have to be considered flexible.

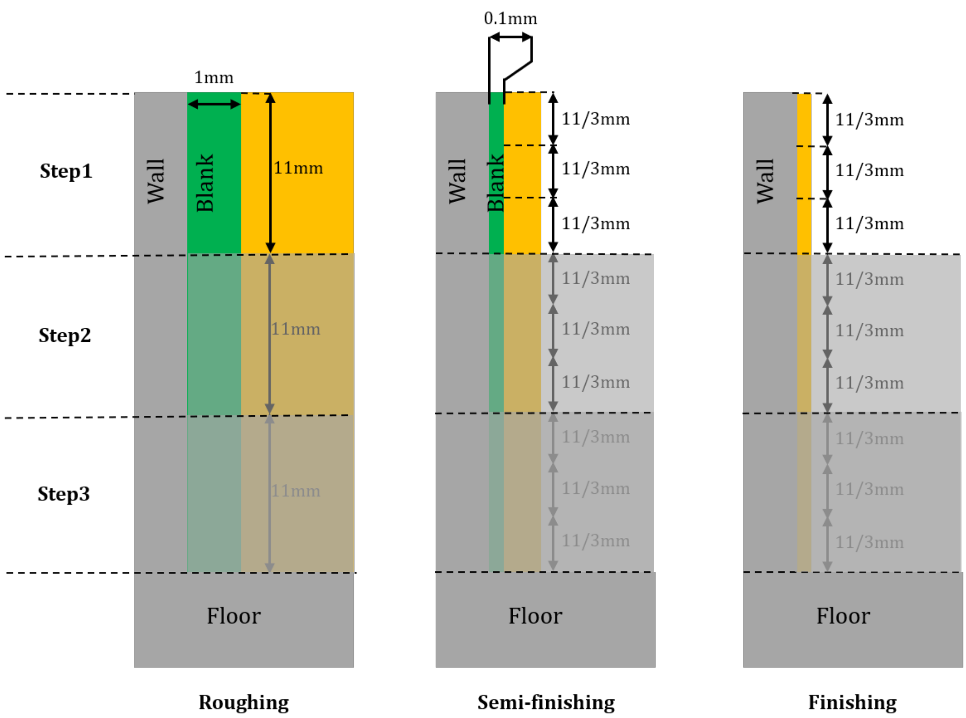

Figure 2.14: Waterline objective strategy

In order to verify if the objective strategy is realistic and to choose stable cutting conditions, three parts respectively cut 11mm, 22mm and 33mm deep were created and modal analysis was performed on them (cf. figures 2.15, 2.16 and 2.17). The procedure is then the following, given for the example of the first step (11mm deep).

After modal analysis is achieved, a harmonic response around the modes locations with a 1Hz sampling frequency gives access to workpiece FRFs of the three modes studied, for each part.

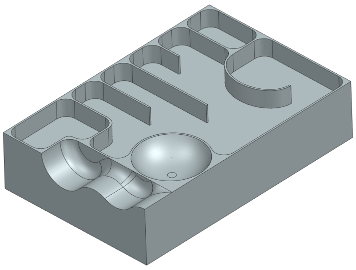

Figure 2.15: Step1

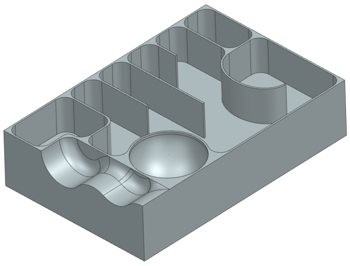

Figure 2.16: Step2

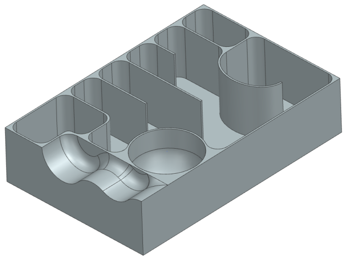

Figure 2.17: Step3

With the help of CutPro, the roughing stability lobes are obtained by imputing the tool FRFs. The fixed parameter is the 11mm depth of cut and outputs are a spindle speed and a width of cut.

For the semi-finishing, both the workpiece and the tool FRFs have to be applied to the CutPro simulation, since the two bodies flexibilities have to be considered. Again, a spindle speed and a width of cut have to be selected for the fixed 11mm depth of cut.
After that, by making the assumption that the workpiece FRF does not change between finishing and roughing and given the 0.1mm radial engagement, a spindle speed and a depth of cut are chosen for the finishing operation.

In the case where no parameter couples are available to ensure stability during an operation, the depth of cut has to be reduced and the process done again. This method leads to the identification of an optimal height-over-thickness ratio for each step and operation.

By applying this procedure to the thin-walled part, the optimal cutting levels were identified and are represented on the picture 2.18.

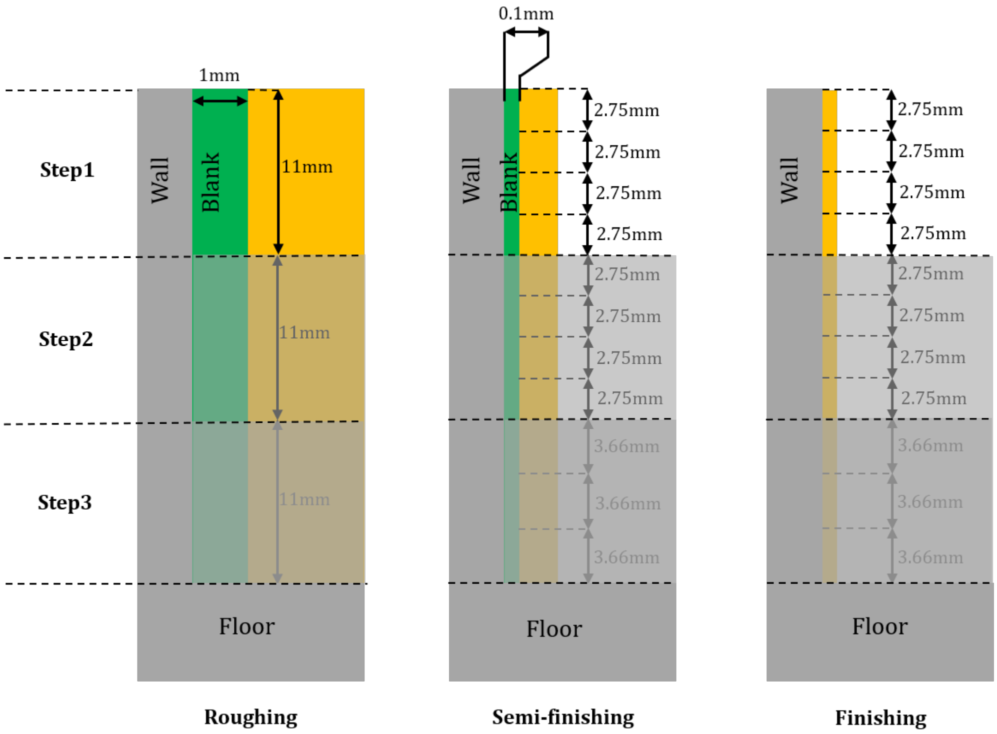

Figure 2.18: Waterline optimized stable strategy

At each cut level, the height-to-thickness ratio is low enough not to consider thin-wall machining, meaning that only the tool flexibility can be taken into account.

The total machining time was recorded at 58 minutes, and chatter was successfully eliminated throughout the operation, as shown in Appendix E. These results demonstrate the effectiveness of the chosen parameters and strategy.

For further optimization, a study could be conducted by using non-uniform passes. The height-to-thickness ratio could be better tuned and the productivity increased.

Chapter 3

Blade machining

In this chapter, comparisons will be made between the performance of different tools during blades machining.

Contents

1 Design

In order to compare the performance of a barrel tool with a ball end mill during thin-wall machining, a postdoctoral student of the laboratory conducted research on a blade project.

Assisting him, my role was to design an assembly of six identical airfoil shapes called blades. Designing six blades enabled us to simulate spatial boundaries during the cutting by limiting accessibility with the presence of adjacent blades. I first had to design blades before programming the CAM for the ball end mill and barrel tool.

For the design, I created an airfoil using a normalized NACA 5310 shape as depicted in the figure below (5% max camber, 30% max camber position, 10% thickness).

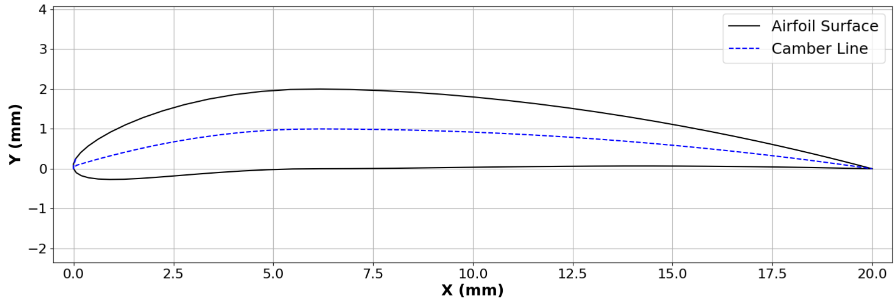

Figure 3.1: Airfoil shape NACA 5310

As it stands, the trailing edge is not machinable because the thickness tends to zero, introducing heavy chatter during the cut. Hence, it has to be blended. Leading and trailing edges also have to be avoided during the machining process.

To overcome this problem, designing shapes with non-constant offsets around the original geometry as illustrated hereafter was a good solution. These offsets are used as final geometry for the ball end mill roughing and semi-finishing. To add a $10mm$ helix angle to the blade, I created a $40mm$ offset of these geometries and applied a rotation.

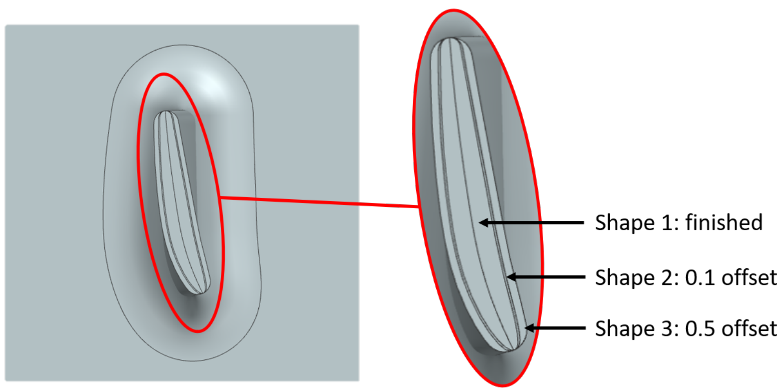

Figure 3.2: Offset airfoil blank shapes

The machine and material used are identical to the previous thin-walled study.

2 Computer-Aided Manufacturing

Regarding the CAM, the main difficulty relies in choosing correct tilt and lead angles to be able to cut the blade despite the restriction of cutting area. A compromise also has to be found when choosing a small depth of cut allowing low scallops while keeping a reasonable machining time. More passes lead to a better surface finish but also mean more time needed to simulate and machine the tool path.
The selection of optimal parameters for Blades CAM is a very time consuming process and can take days of work.

The next step is to chose stable cutting conditions. Both the part and the tool have to be considered flexible. For this reason, the postdoctoral student performed FEA on the camber surface of the blades. We then proceeded to a tap test on the tool. When using a soft rubber tip on the impact hammer, the interesting modes were not excited with a sufficient magnitude. Consequently, we employed a metal tip, which caused double hits. We also chipped the tool flute by hitting too hard.

After the roughing and shape 3 semi-finishing operations (see figure 3.2), the workpiece is flexible and close to the finished geometry. At this point, we are in the right configuration to proceed to a tap test.

Hitting the workpiece with a hammer is challenging, if not impossible due to its low thickness. The solution was to use an automatic impact hammer and laser velocity sensor as for the thin-walled part to get the modes of the machined part (see figure 3.3).

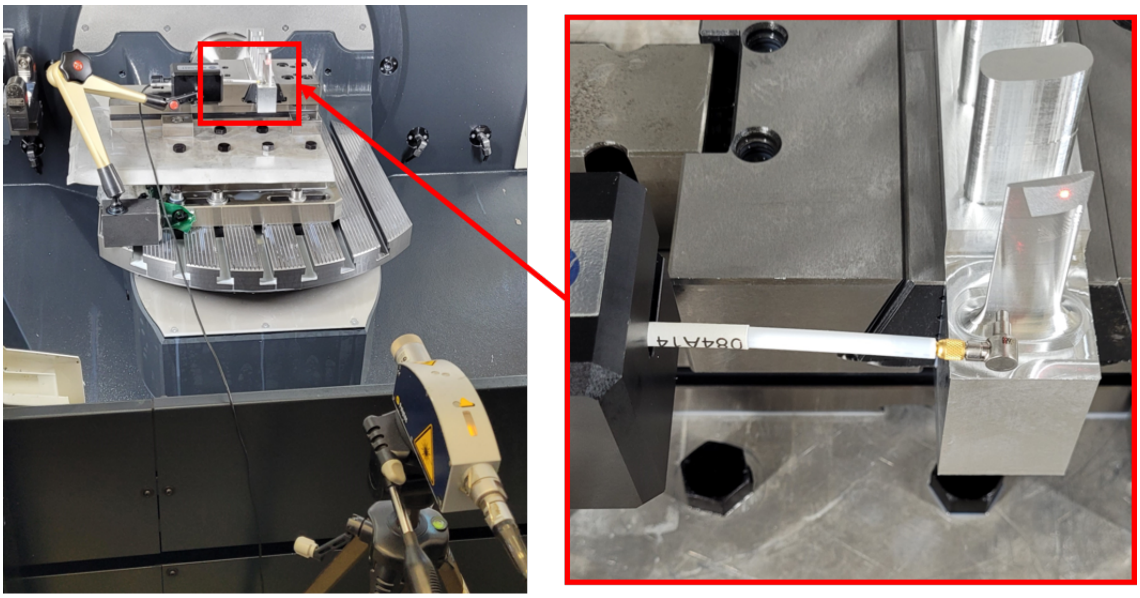

Figure 3.3: Automatic tap testing setup

Even with the automatic hammer, it was impossible to perform the test on top of the

blade because of systematic double hits. By applying the impact on the middle of the blade, we were able to successfully single hit the structure and measure the damping ratio to tune the FEA.
We than combined results with tool tap testing results to choose stable cutting conditions from both the tool and the workpiece from stability lobes.

NX software does not include machine characteristics. Thus, tool motions can be wrongly represented during simulation, especially during 5-axis operations. To meet this challenge, the laboratory uses Vericut. This software requires the same imputs as NX, as well as the machine characteristics to simulate motions. After simulating the machining process, the gouge and excess option allowed me to observe the overcut and leftover regions, respectively in red and blue (cf. figure 3.4).

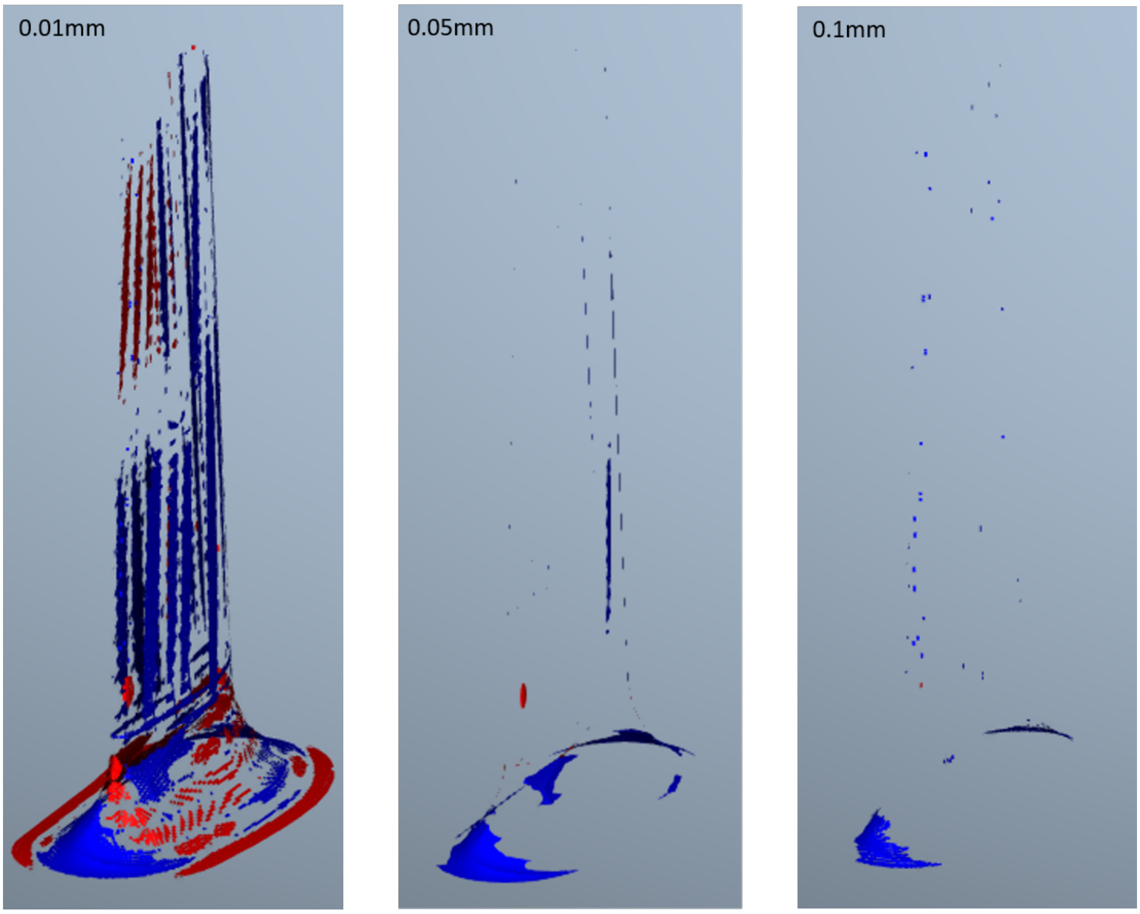

Figure 3.4: Vericut gouge and excess for different thresholds

The most noticeable excess is located on the edge blend. However, the blend is not the most functional geometry of the part and is not essential for the study. Therefore, this area does not need to be accurately cut.

This procedure was repeated for other adjacent blades with different strategies:

- 1st blade: waterline approach with ball end mill, height divided in three to reduce chatter risk ;
- 2nd blade: regular approach with ball end mill ;
- 3rd blade: regular approach with barrel tool ;
- other blades: strategies to be chosen after previous results.

During the cut of the first blade, slight chatter was observed. This indicates that with regular approaches the part will be prone to chatter at higher amplitudes. To address this, a tap test can be performed on the part before semi-finishing it with the ball end mill in order to tune the spindle speed and avoid vibration modes. However, if the system's static stiffness is too low, it may be impossible to find stable cutting conditions. Static stiffness can be accessed by applying a known static load to the blade and measuring the resulting displacement.

3 Machining

After machining, we can notice that the waterline approach is necessary to cut thin blades. The second and third blades, that were cut with a conventional approach, were subject to highly destructive chatter as illustrated in the figure 3.5.

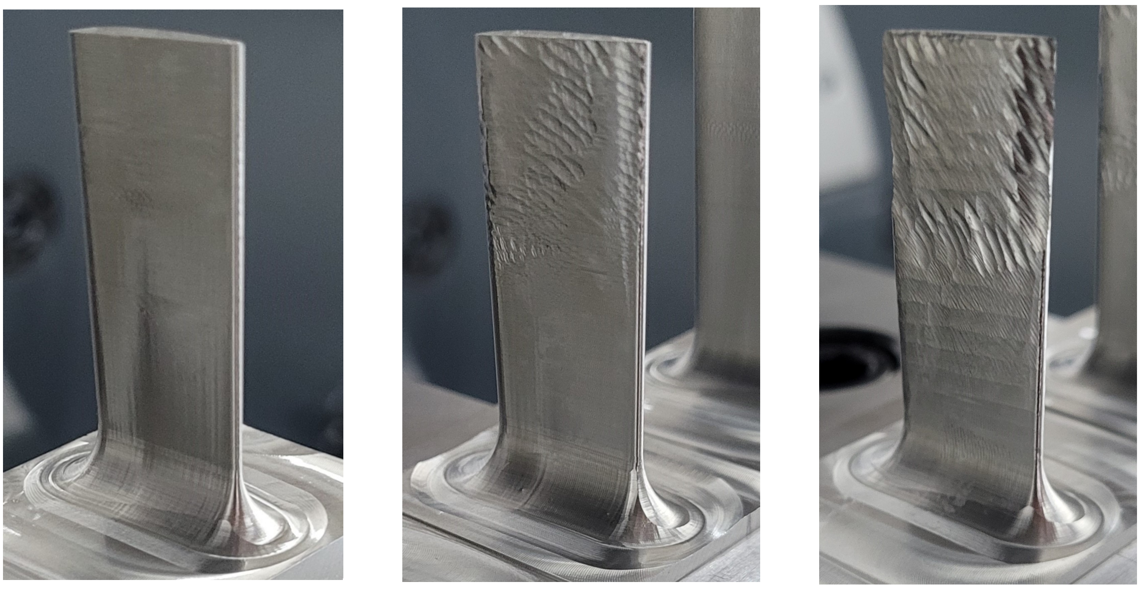

Figure 3.5: 1st, 2nd and 3rd blade machined (from left to right)

Applying an optimized waterline approach and adapting the depth and width of cut might reduce chatter and thus improve surface finish.

Conclusion

This internship was the opportunity for me to discover research in an internationally renowned manufacturing laboratory. Working alongside engineers, PhD students and postdoctoral researchers enhanced my understanding of machining processes and strengthened my intention to pursue further studies and my future career in this field.

The study of thin-walled parts offered a good understanding of the challenges of chatter avoidance encountered during slender parts machining. In particular, the waterline strategy optimization is essential for achieving a balance between chatter stability and productivity. The method developed in this study successfully lead to the elimination of chatter on the part. The applications of this study are numerous, especially in the aeronautics and space industries, where thin-walled components such as blades are often manufactured.

Future improvements to this study could be achieved with the use of non-uniform depths of cut, which could further optimize the cutting conditions. Once the optimal height-to-thickness ratio is found for the studied material, the methodology could be extended to other materials. However, the results of this study are only applicable to the tool and workpiece considered.

Developing a waterline strategy using the method described in this study is particularly valuable for high value-added components. Although the procedure is time-consuming, it provides enhanced stability during the hole cutting process while simultaneously reducing overall machining time, which is especially critical for high-volume production.

Bibliography

[Altintas and Weck, 2004] Altintas, Y. and Weck, M. (2004). Chatter stability of metal cutting and grinding. *CIRP Annals - Manufacturing Technology*, 53:619–642.

[Altintaş and Budak, 1995] Altintaş, Y. and Budak, E. (1995). Analytical prediction of stability lobes in milling. *CIRP Annals - Manufacturing Technology*, 44:357–362.

[Ding and Zhu, 2018] Ding, Y. and Zhu, L. (2018). Investigation on chatter stability of thin-walled parts considering its flexibility based on finite element analysis. *International Journal of Advanced Manufacturing Technology*, pages 3173–3187.

[Özşahin et al., 2010] Özşahin, O., Özgüven, H., and Budak, E. (2010). Analysis and compensation of mass loading effect of accelerometers on tool point frf measurements for chatter stability predictions. *International Journal of Machine Tools Manufacture*, 50:585–589.

[Tehranizadeh et al., 2022] Tehranizadeh, F., Berenji, K. R., Yıldız, S., and Budak, E. (2022). Chatter stability of thin-walled part machining using special end mills. *CIRP Annals - Manufacturing Technology*, 71:365–368.

[Tobias, 1961] Tobias, S. A. (1961). Machine tool vibration research. *International Journal of Machine Tools and Manufacture*, 1:1–14.

Appendix A

Thin-walled part CAD

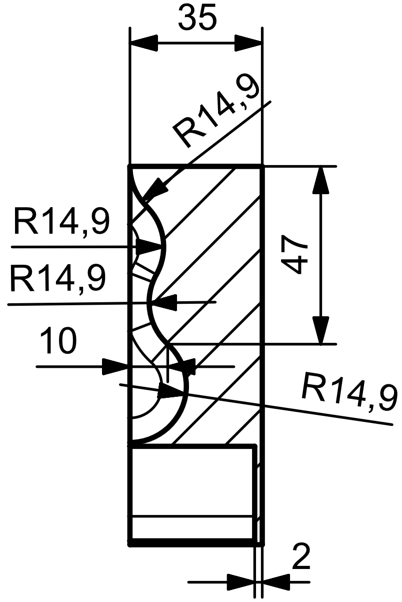

SECTION C-C

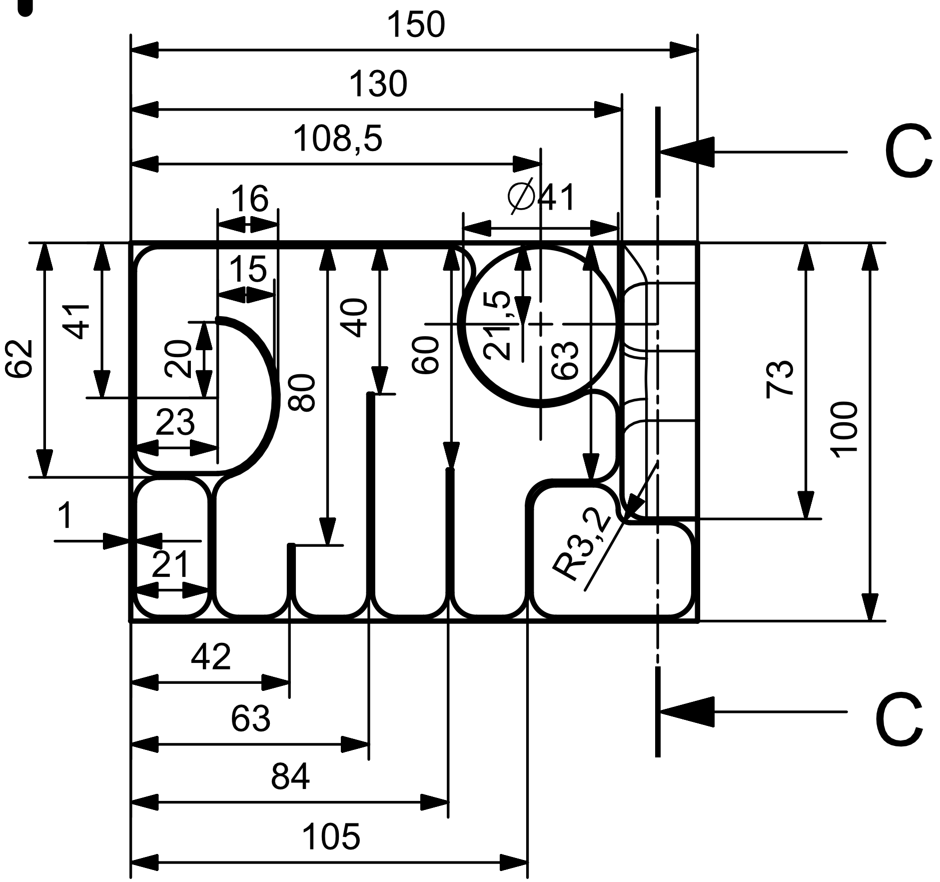

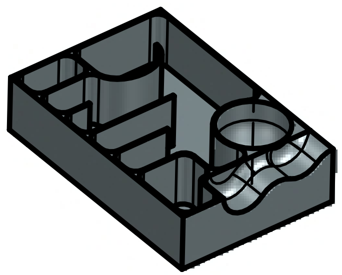

SCALE 1:4

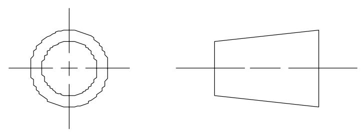

All blend radii are 6.5mm except those specified
Standard thin walls dimension is 1mm

ALL DIMENSIONS IN MM

SIEMENS		THIS DRAWING HAS BEEN PRODUCED USING AN EXAMPLE TEMPLATE PROVIDED BY SIEMENS PLM SOFTWARE		
FIRST ISSUED		TITLE: Thin-walled part		
DRAWN BY	Thomas Fix			
CHECKED BY				
APPROVED BY		SIZE	DRG NO.	SHEET REV
MATERIAL	Al 7050	A4	thin_walled_part_v3_dwg1	A
MACHINE	DMU 50	SCALE 1:2		SHEET 2 OF 2

Appendix B

Chatter marks

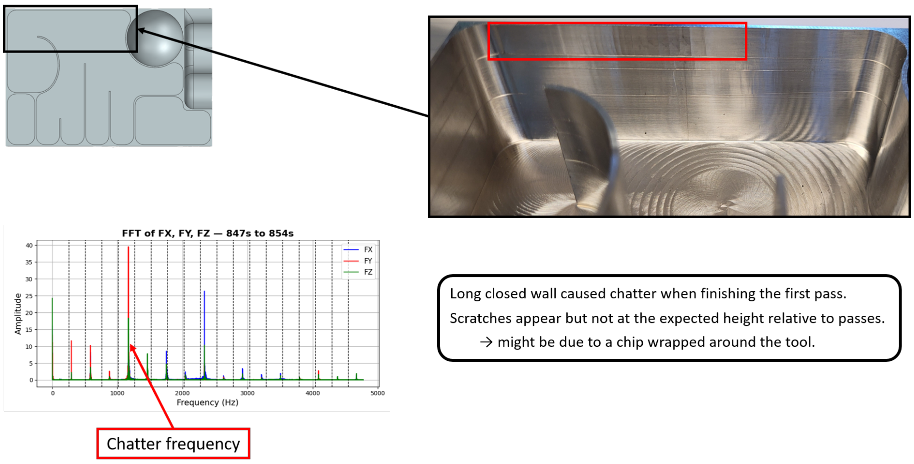

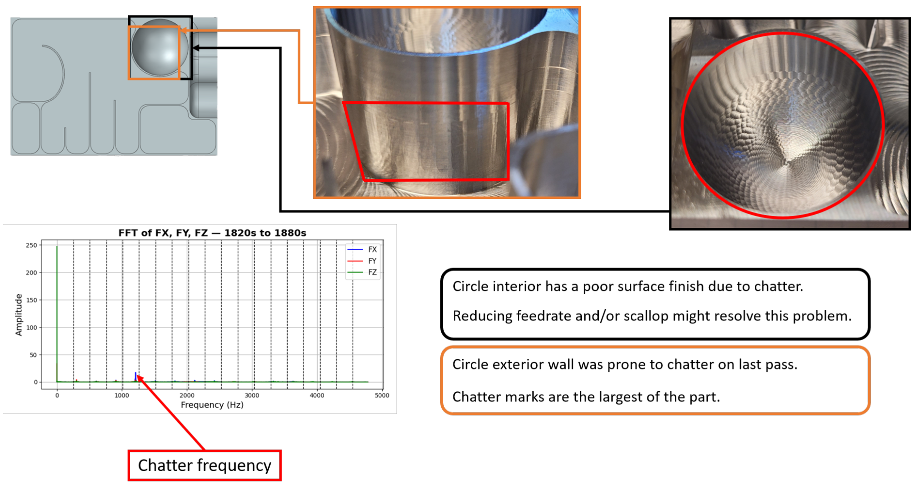

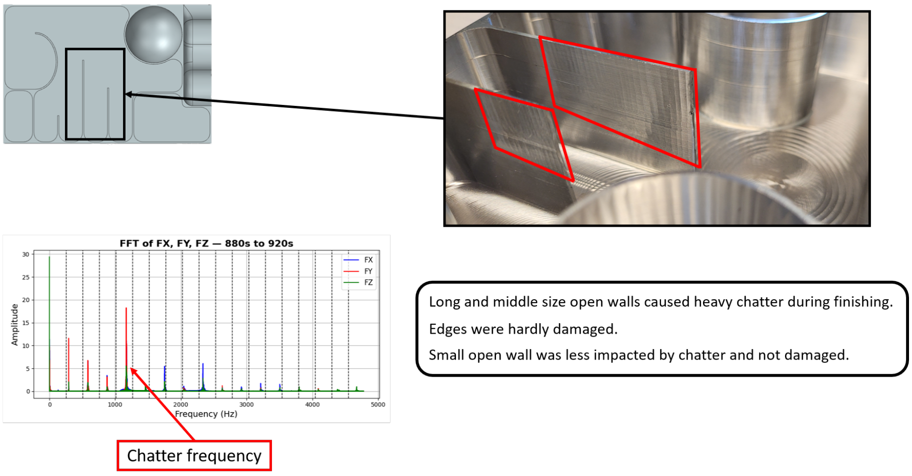
FFT of FX, FY, FZ — 880s to 920s
Long and middle size open walls caused heavy chatter during finishing.
Edges were hardly damaged.
Small open wall was less impacted by chatter and not damaged.
Chatter frequency

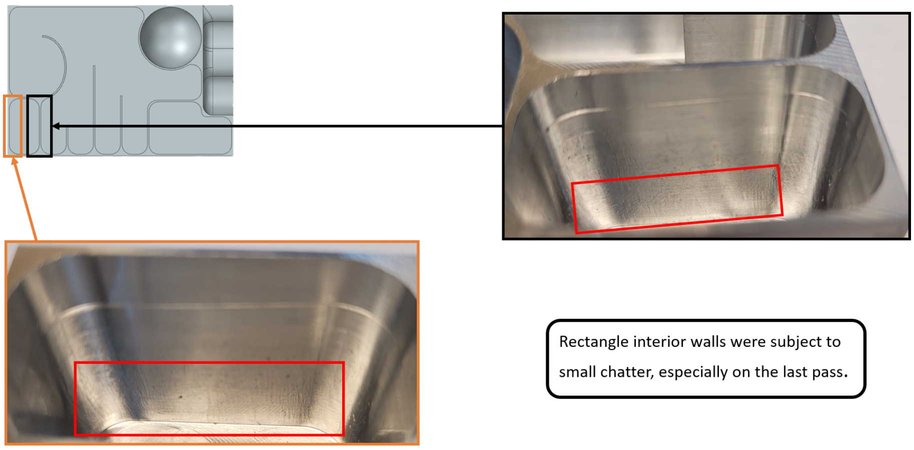
Rectangle interior walls were subject to small chatter, especially on the last pass.

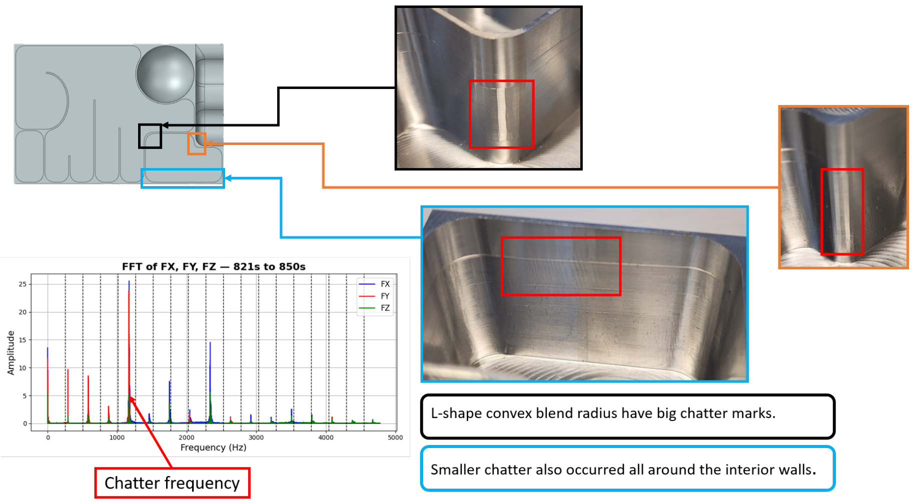
FFT of FX, FY, FZ — 821s to 850s
L-shape convex blend radius have big chatter marks.
Smaller chatter also occurred all around the interior walls.
Chatter frequency

Appendix C

Thin-walled part mode shapes

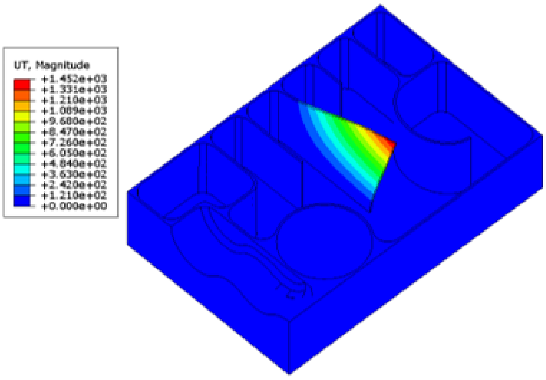

Figure C.1: Mode 1: 1024Hz

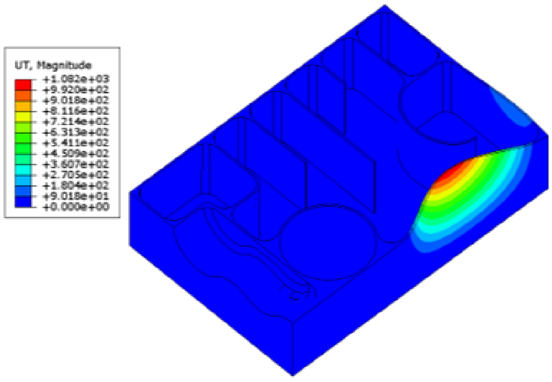

Figure C.2: Mode 2: 1457Hz

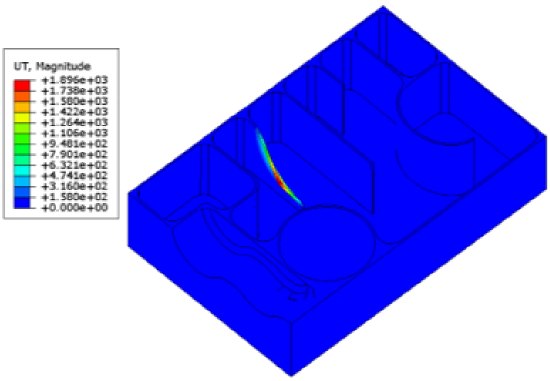

Figure C.3: Mode 3: 1490Hz

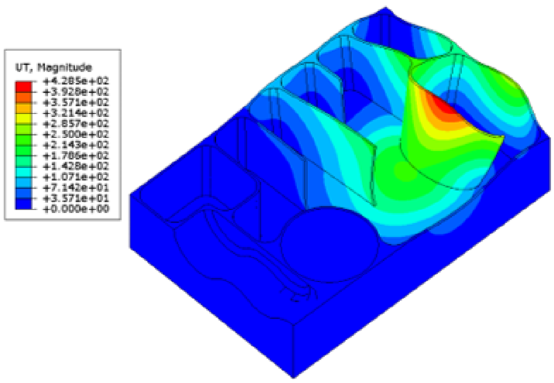

Figure C.4: Mode 4: 1835Hz

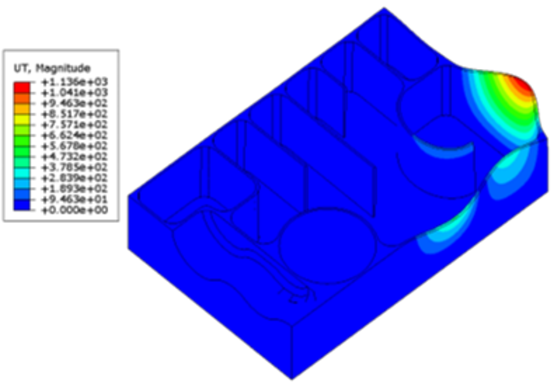

Figure C.5: Mode 5: 2276Hz

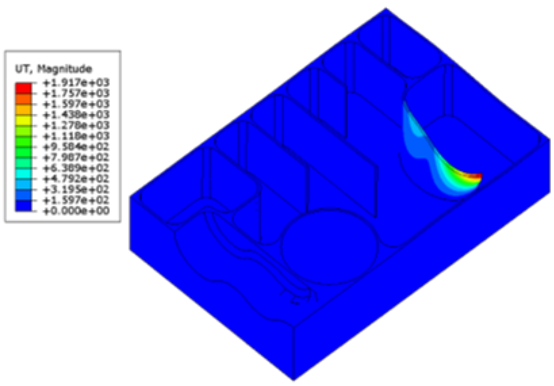

Figure C.6: Mode 6: 2463Hz

Appendix D

FEA model tuning

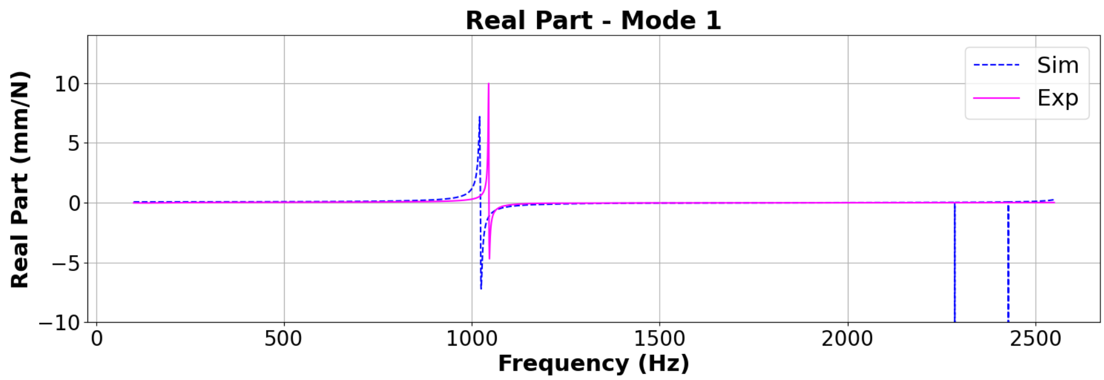

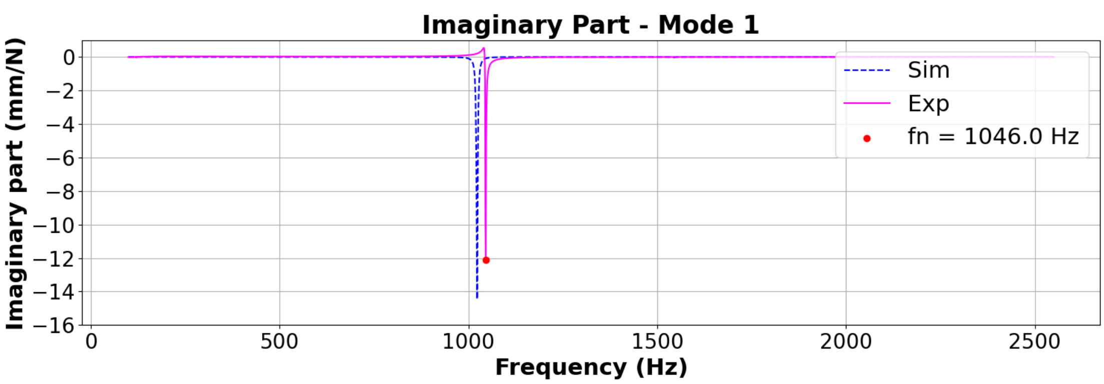

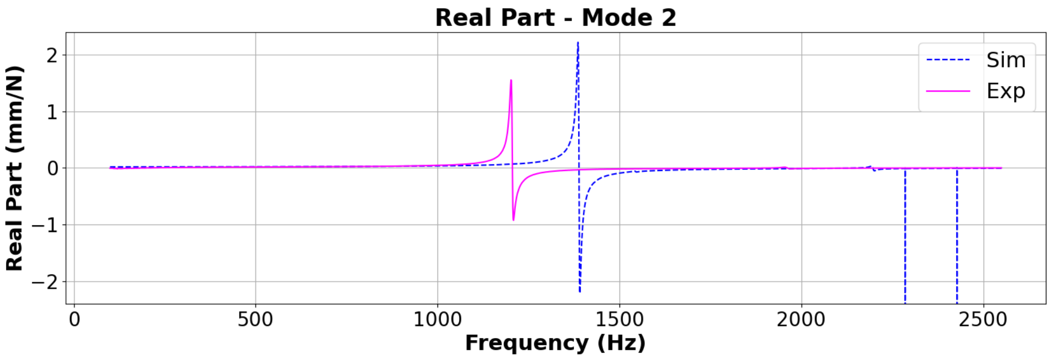
Real Part - Mode 2
Sim
Exp
Real Part (mm/N)
2
1
0
−1
−2
0
500
1000
1500
2000
2500
Frequency (Hz)

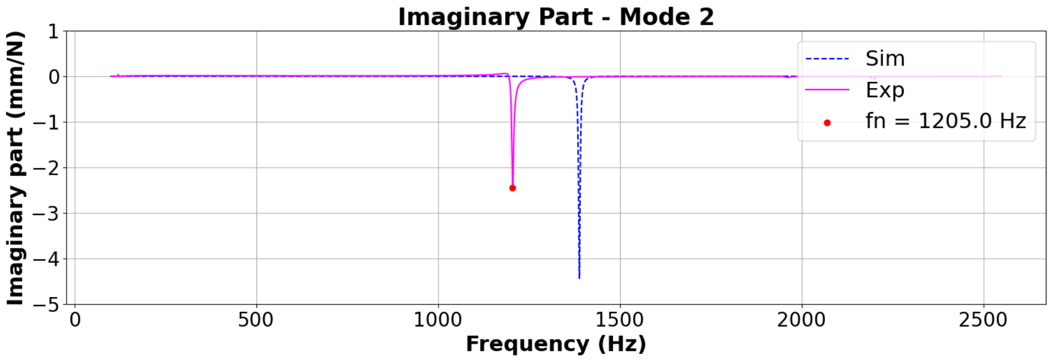
Imaginary Part - Mode 2
Sim
Exp
fn = 1205.0 Hz
Imaginary part (mm/N)
1
0
−1
−2
−3
−4
−5
0
500
1000
1500
2000
2500
Frequency (Hz)

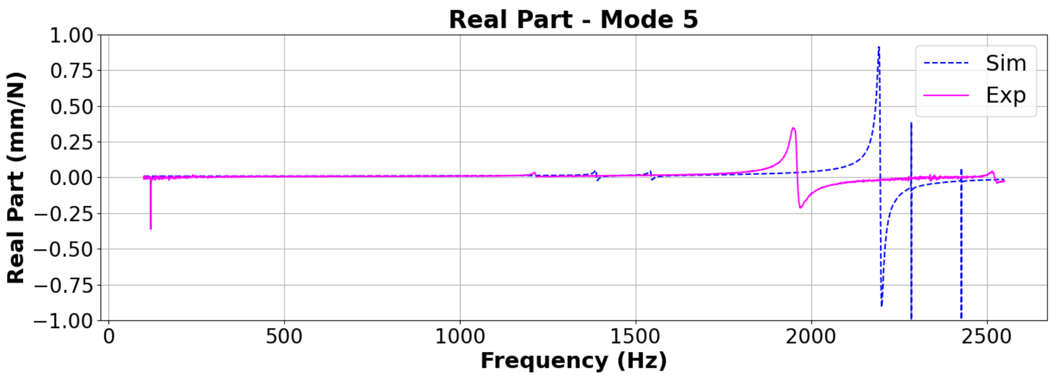
Real Part - Mode 5
Sim
Exp
Real Part (mm/N)
1.00
0.75
0.50
0.25
0.00
−0.25
−0.50
−0.75
−1.00
0
500
1000
1500
2000
2500
Frequency (Hz)

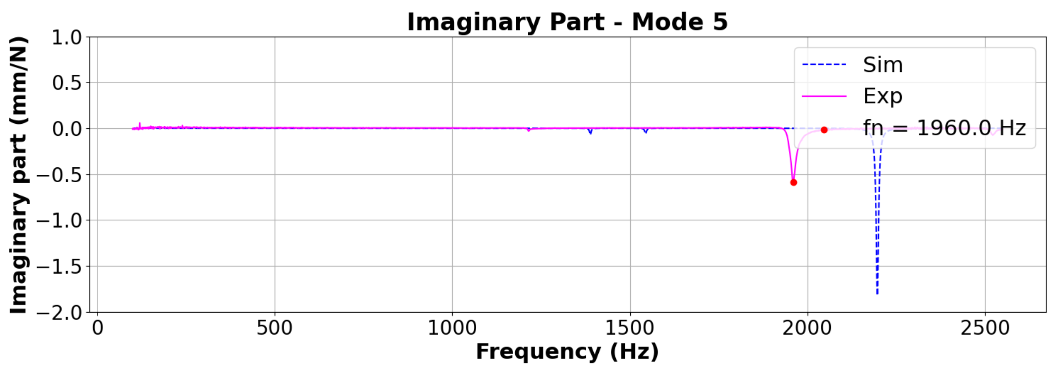
Imaginary Part - Mode 5
Sim
Exp
fn = 1960.0 Hz
Imaginary part (mm/N)
1.0
0.5
0.0
−0.5
−1.0
−1.5
−2.0
0
500
1000
1500
2000
2500
Frequency (Hz)

Appendix E

Waterline optimized strategy results